Available online at www.sciencedirect.com
SCIENCE DIRECT®
Journal of Power Sources 150 (2005) 101–109
JOURNAL OF POWER SOURCES
www.elsevier.com/locate/jpowsour

Dynamic simulation model of a steam reformer for a residential fuel cell power plant

Hans-Jürgen Jahn*, Wolfgang Schroer

Fachhochschule Ulm, IAF Automatisierungssysteme, Postfach 3860, D-89075 Ulm, Germany

Received 7 November 2004; accepted 14 February 2005
Available online 29 April 2005

Abstract

This paper presents a lumped element model of a natural gas steam reformer being part of a 5 kW(el.) residential fuel cell power plant. It describes the thermal behaviour over the whole operating range including plant startup. For the reforming reactions chemical equilibrium is assumed. The derivation of the model starting with basic thermal and chemical laws is shown. Therefore model parameters have a physical meaning and were calculated with the assumption of lumped system properties. To achieve a better agreement with experiments the parameters were furthermore identified from measured data. Experimental data of a demonstration plant were used to verify the model.
© 2005 Elsevier B.V. All rights reserved.

Keywords: Steam reforming; Dynamic model; Fuel cell power plant; Chemical equilibrium

1. Introduction

Fuel cell power plants are a promising technology: Using hydrogen as fuel they provide a local emission free energy source with high electrical efficiency. To increase overall efficiency also the waste heat should be used in a combined heat and power plant. Therefore currently small power plants for residential energy supply are developed which should replace the conventional heating system. But due to the lack of a hydrogen infrastructure the already available natural gas is the fuel for the near future. If using natural gas, hydrogen is produced by a reforming process.

Recent developments show the feasibility of such small units and some demonstration plants already exist. Up to now only very limited data of these plants, including the reforming process, are published.

In this paper a dynamic model of a steam reformer for a residential fuel cell system is presented. The model was constructed using basic physical and chemical laws and therefore provides a good insight into the process and covers the complete operating range including startup and shutdown. This considerations may be used also for different reformer types.

Our applications are control system design and the optimization of the plant startup procedure. The first application can be divided into controller design and observer design: For controller design the model is only applied offline during the design process. In difference, in an observer the model is applied online, i.e. it runs in parallel to the real plant and is used to estimate plant data. This may be the outlet gas composition which can not be measured directly with acceptable expense under real operating conditions. The second application, optimization of plant startup, is targeted on the calculation of control inputs that minimize some objective function. Therefore a model of the whole plant, with the reformer as one component, is required.

In the first part of this paper the demonstration plant is described. In the second part the model structure, assumptions and simplifications are discussed. The third part covers the theoretical calculation and identification of the model parameters and finally the model is compared with real plant data.

2. Demonstration plant

The described reformer is shown in Fig. 1. It is part of a demonstration plant of a residential fuel cell power station

* Corresponding author.
E-mail address: jahn@fh-ulm.de (H.-J. Jahn).

0378-7753/$ – see front matter © 2005 Elsevier B.V. All rights reserved.
doi:10.1016/j.jpowsour.2005.02.012

Nomenclature

C	heat capacity ($c \cdot m$)
c	specific heat capacity
G	Gibbs enthalpy
g	specific Gibbs enthalpy
Δh	heat of reaction
k	factor for heat conduction/radiation
m	mass
n	amount of substance
Δn	extent of reaction
$\dot{n}$	molar flow rate
p	pressure
p_0	standard pressure
$\underline{p}$	parameter vector
$\dot{Q}$	heat flow
R	gas constant
r	heat of evaporation
S/C	steam to carbon ratio
s	valve position
T	temperature
$\underline{u}$	parameter vector
y	concentration
λ	excess air value

Indices

A	ambient
B	burner
c	convection
E	evaporator
e	evaporation
F	flame
G	ground plate
i	inlet
o	outlet
R	reactor
r	reaction
V	burner valve
W	wall

located at the Fachhochschule Ulm. The plant was developed by the Centre for Solar Energy and Hydrogen Research (ZSW), Ulm, and the gas processing subsystem (described in [1]) by the Fraunhofer Institute for Solar Energy Systems (ISE), Freiburg.

The plant components are shown in Fig. 2. Natural gas and water are fed to the reformer which is heated by a natural gas burner. The product gas is a mixture containing mainly hydrogen, carbon dioxide, some methane and also carbon monoxide in the range of a few percent. As carbon monoxide acts as a catalyst poison for the fuel cell, it is removed in a gas purification system consisting of two shift stages and a PROX-unit. Before entering the fuel cell stack the gas is humidified. The stack is a 40 cell PEM type with 5 kW(el.)

Fig. 1. The steam reformer. Approximate dimensions are 60 cm height and 28 cm diameter.

nominal power. The hydrogen which is not consumed in the cell is fed to a catalytic burner.

A detailed cross-section of the reformer is depicted in Fig. 3. Natural gas (methane) and liquid water enter the evaporator section at the top and flow to the center inside a helical tube. The gas and water are heated by the hot flue gas from the gas burner. The methane/steam mixture then enters the reactor consisting of an inner and outer tube filled with catalyst material. At the catalyst the following two reactions take place at temperatures above 500 °C [2]:

$$CH_4 + H_2O \rightleftharpoons CO + 3H_2 \qquad \Delta h_0 = 206\,\text{kJ/mol} \tag{1}$$

$$CO + H_2O \rightleftharpoons CO_2 + H_2 \qquad \Delta h_1 = -41\,\text{kJ/mol} \tag{2}$$

The outlet composition depends on the operating conditions and is typically about 10% CO_2, <10% CO, a few percent CH_4 and the remainder H_2 (dry gas). The overall reaction is endothermic. The reaction heat is provided by a natural gas burner located around the reactor tubes. Natural gas and air are mixed outside the burner and flow through perforated ceramic plates. The combustion takes place at the inner plate surface:

$$CH_4 + 2O_2 \longrightarrow CO_2 + 2H_2O \qquad \Delta h_C = -804\,\text{kJ/mol} \tag{3}$$

The flue gas flows through the gap between the two reactor tubes and then through the evaporator. Therefore the reactor is heated by radiation from the burner plates and convection of the flue gas.

The inlet (CH_4) gas flow rate can be varied between 10 and 25 SLPM (standard liter per minute). The water flow rate is given through the molar ratio of water to methane (steam to carbon, S/C) which is approximately 3.5. Temperatures are measured at the evaporator outlet, the reactor outlet and at four different locations of the burner using

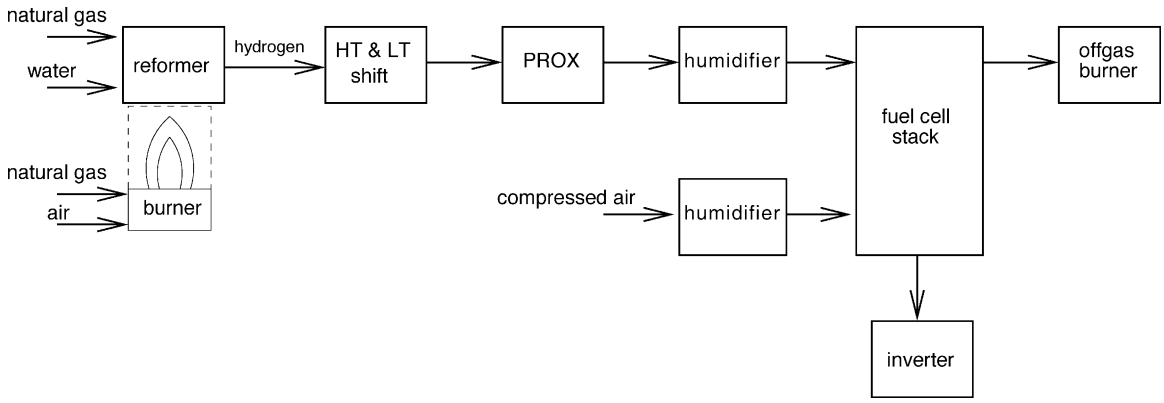

Fig. 2. Components of the demonstration plant.

K-type thermocouples. The outlet gas composition is analyzed with an Emerson NGA2000 process gas analyzer (containing NDIR-(infrared-)sensors for CO_2, CO, CH_4 and a heat conduction sensor for H_2).

The plant is controlled by an industrial programmable logic controller (PLC). For the reformer system it calculates the natural gas and water flow rates and controls the burner temperature. The reforming gas flow rate is set with a speed controlled compressor and the water flow rate with a dosing pump.

The experimental data comprise two different operation points, i.e. 40 and 70 SLPM reformate flow, each with stepwise variations in gas and water flow rates and burner temperature. The operating pressure is 3.5 bar.

3. Reformer model

Inputs and outputs of our model are listed in Table 1. Before continuing with its description some common approaches shall be shortly reviewed. Models of dynamic systems can be divided into theoretical and experimental ones [3]. Theoretical models rely on physical equations and therefore they describe the inner structure of a system. Usually they are expressed as differential equations.

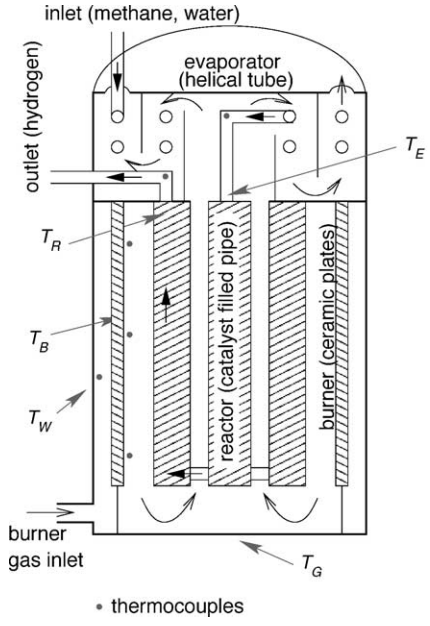

Fig. 3. Cross-section of the reformer.

In contrast experimental models are based on measured data (e.g. the step response) and therefore they describe the relation between inputs and outputs, but not the inner structure of a system. Based on the experimental data the parameters of some standard structure (e.g. a transfer function) may be calculated. This is called fitting or identification and the result is a parametric model [4].

In practice often some intermediate approaches are used, for example, the structure of a parametric model results from theoretical modeling but its parameters are identified based on experimental data.

Examples are Meziou and Alatiqi [5], which describe the development of a control system for an industrial steam reformer. First they give a theoretical model of this reformer and identify its parameters based on experimental data. Then, for control system design, they derive a linear ARX model from the initial model (ARX is a standard structure consisting of a discrete time, rational transfer function and delay time). Such a model is well suited for control system design if operating conditions are close to the one used during identification, but we also need to describe the reformer startup.

An example of a theoretical steam reformer model can be found in [6]. This paper describes a tubular fixed bed reactor and considers reaction kinetics, diffusion and heat conduction. This results in a two-dimensional partial differential equation (PDE). For simulation a finite-difference discretization is applied. This model only includes the reactor itself but no further components like evaporator and burner. A one-dimensional model of an auto-thermal methanol reformer for automotive use is described by Maume [7]. We do not use a PDE structure because of the much more complex geometry of our system and because simple ordinary differential equation (ODE) models are preferred for control system design.

General information on the chemistry of steam reforming can be found in [8] and targeted to fuel cell systems in [2].

Table 1
Model inputs and outputs

Inputs	
–	Burner state (fan on/off, gas valve open/closed)
s_V	Burner valve position
$\dot{n}_{H_2O}$, T_{H_2O}	Water flow rate and temperature
$\dot{n}_{CH_4}$, T_{CH_4}	Natural gas flow rate and temperature
Outputs	
T_W	Wall temperature
T_B	Burner temperature
T_E	Evaporator temperature
T_R	Reactor temperature
$\underline{\dot{n}}_R$	Outlet gas flow (CH_4, H_2O, H_2, CO_2, CO)

The physical laws are generally represented as partial differential equations. But to ensure later applicability for control system design and also as observer in an operational system a lumped model structure in the form of ODEs is used.

The lumped elements are wall, ground plate, burner, reactor and evaporator. Each of them is assigned one uniform temperature:

- wall (temperature T_W): This is the tube around the burner. The corresponding temperature sensor is mounted between the wall and the burner and indeed measures the temperature of the burner gas, which is assumed to adopt the wall temperature.
- ground plate (T_G): The steel plate at the bottom of the reformer assembly. Its temperature is not measured.
- burner (T_B): The burner consists of ceramic plates located around the reactor. The temperature sensors are near the plate surface where combustion takes place. It is assumed that the sensors correspond to the surface temperature.
- evaporator (T_E): It is the top part of the reformer. Here the outlet temperature (equal to the reactor inlet temperature) is of interest.
- reactor (T_R): It is located in the center of the burner. There is no temperature sensor inside the reactor, but as the gas composition depends on the reactor temperature (discussed below), the reactor temperature is defined by the corresponding outlet gas composition. A temperature sensor located at the reformer outlet only approximately agrees with the actual reactor temperature, especially not during dynamic operation (e.g. plant startup).

In the following the heat exchange mechanisms between the above elements are discussed (see also Fig. 4):

- Heat conduction is modeled as proportional to the temperature difference with a proportionality factor *k*. *k* results from geometry and heat conductivity and is constant (i.e. not temperature dependent). The heat transfer from the evaporator to the ambience consists of conduction in the thermal insulation and free convection. These two effects are not modeled separately.
- Radiation takes place between burner and reactor. The heat flow is proportional to the difference of the 4. power of the temperatures with the proportionality factor k_{BR} describing geometry and surface emissivity (which is assumed to be temperature independent). Radiation from burner to wall is negligible, because the outside surface temperature of the burner plates is much lower than their inside temperature. The temperature gradient over the burner cross-section [9] is not taken into account.
- Convective heat transfer is considered for both burner and reformate gas streams. But its calculation is only feasible for simple geometries [10]. Therefore and to keep the model simple it is assumed that gas flowing through or along an element adopts the element temperature. Then the heat flow can be calculated from an energy balance. There is only one exception: It is not likely that the flue gas cools down to the ground plate temperature. Therefore here a constant k_{FG} is introduced, which corresponds to

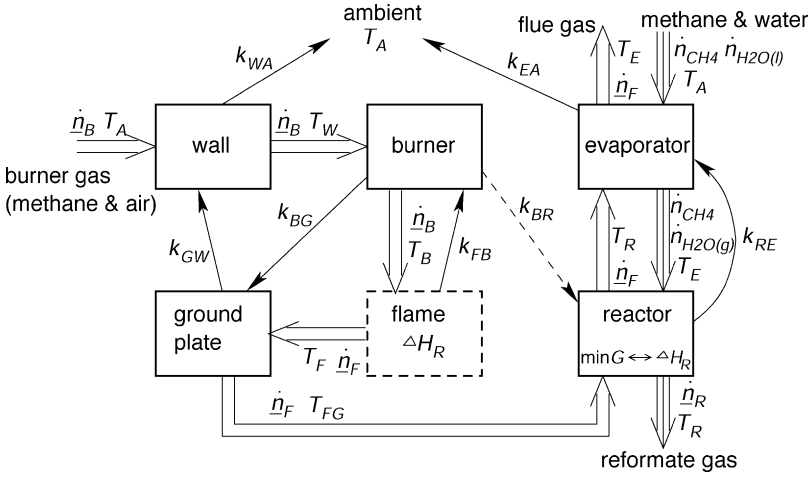

Fig. 4. The model structure: The boxes correspond to the lumped elements, single lines depict heat transfer (solid: conduction, dashed: radiation), double lines depict the burner gas flow and triple lines the reformate gas flow.

the fraction of heat transferred. So the flue gas cools down to $T_{FG} = T_F - k_{FG}(T_F - T_G)$.

- The combustion takes place at the surface of the burner which is heated by the hot flue gas. This heat flow is assumed to be proportional to the difference of flame and burner temperature.
- Methane and water (liquid) entering the evaporator are heated up to the evaporator temperature, i.e. the water evaporates.
- The methane steam mixture leaving the evaporator with T_E enters the reactor and is heated up to the reactor temperature T_R. The reaction takes place at this temperature.

There are two approaches for the calculation of the outlet gas composition. The first is based on reaction kinetics (used in [6,7,11]) and requires the solution of a ODE system, while the second assumes chemical equilibrium ([12]) and leads to a nonlinear algebraic equation. We use the second method and achieve reasonable results for the flow rates applied in our system. Of course at higher flow rates the influence of reaction kinetics would become apparent, but this is not within the operation range of our system.

The equilibrium composition is defined by minimal free enthalpy. Its practical calculation is explained briefly. Because no analytical solution exists and the numerical solution is computationally expensive, also an approximate solution is presented. This is better suited for online application as part of a plant control system with limited computation resources and real-time requirements.

Consider a gas mixture with all N components of the reforming reactions (1, 2) at constant pressure p, temperature T_R and initial composition $n_{CH_4,i}$ and $n_{H_2O,i}$ (Natural gas may contain considerable amounts of other gases including hydrocarbons other than methane). For our gas supply this is not the case. Otherwise these further components must be included in the free enthalpy calculation and maybe other reactions than (1) and (2) can take place). As the two reactions are independent, all possible compositions can be expressed using the extent of reaction Δn_0 and Δn_1:

$$\underline{n}_R = \begin{pmatrix} n_{CH_4,R} \\ n_{H_2O,R} \\ n_{H_2,R} \\ n_{CO_2,R} \\ n_{CO,R} \end{pmatrix} = \begin{pmatrix} n_{CH_4,i} \\ n_{H_2O,i} \\ 0 \\ 0 \\ 0 \end{pmatrix} + \Delta n_0 \begin{pmatrix} -1 \\ -1 \\ 3 \\ 0 \\ 1 \end{pmatrix} + \Delta n_1 \begin{pmatrix} 0 \\ -1 \\ 1 \\ 1 \\ -1 \end{pmatrix} \tag{4}$$

Here n denotes the amount of substance. The range of Δn_0 and Δn_1 is restricted by the condition $n_i \geq 0$. With these definitions the free enthalpy G can be written as ([13]):

$$G\{\Delta n_0, \Delta n_1\} = \sum_{i=1}^{N} n_{i,R} \left(g_i\{T\} + RT \ln \frac{p_i}{p_0} \right),$$

$$p_i = p \frac{n_{i,R}}{\sum_{i=1}^{N} n_{i,R}}$$

The equilibrium corresponds with the minimum of $G\{\Delta n_0, \Delta n_1\}$ which is denoted by G^*:

$$G^*\{\Delta n_0^*, \Delta n_1^*\} = \min_{\Delta n_0, \Delta n_1} G \tag{5}$$

The minimum is determined numerically using an optimization method based on a random search algorithm with initial conditions $\Delta n_0 = \Delta n_1 = 0$. The transition to molar flows is straightforward by replacing n by $\dot{n}$. The equilibrium calculation was verified with data from [2] and [8].

Also a polynomial approximation for the equilibrium with a structure based on the two-dimensional Taylor series was derived. Operation at constant pressure is assumed and therefore the pressure dependence is ignored. The approximation $\{\Delta\hat{n}_0^*, \Delta\hat{n}_1^*\}$ is only valid within a certain temperature and S/C-range:

$$\begin{aligned} \Delta\hat{n}_0^* &= \underline{p}_0 \cdot \underline{u} \cdot n_{H_2O,i} \\ \Delta\hat{n}_1^* &= \underline{p}_1 \cdot \underline{u} \cdot n_{H_2O,i} \end{aligned} \tag{6}$$

with

$$\underline{u} = (1 \quad \alpha \quad \alpha^2 \quad \alpha^3 \quad \beta \quad \beta^2 \quad \beta^3 \quad \alpha\beta \quad \alpha^2\beta \quad \alpha\beta^2)^T \tag{7}$$

$$\alpha = \frac{T_R}{100K} - 9 \tag{8}$$

$$\beta = \frac{n_{H_2O,i}}{n_{CH_4,i}} - 3.5 = \frac{S}{C} - 3.5 \tag{9}$$

Scaling of S/C and T_R is optional but improves numerical accuracy. The parameters $\underline{p}_0$ and $\underline{p}_1$ were fitted with the least squares method for $p = 3\,\text{bar}$, $S/C = [2; 5]$ and $T_R = [500\,^\circ\text{C}; 800\,^\circ\text{C}]$:

$$\begin{aligned} \underline{p}_0 = (&195.0 \ \ 88.22 \ \ -5.504 \ \ -9.538 \ \ -30.41 \ \ 7.821 \\ &-2.223 \ \ -27.16 \ \ -4.443 \ \ 7.684) \cdot 10^{-3} \end{aligned} \tag{10}$$

$$\begin{aligned} \underline{p}_1 = (&134.5 \ \ 14.02 \ \ -19.62 \ \ 2.491 \\ &-11.94 \ \ 0.09909 \ \ 0.3631 \ \ 0.7817 \ \ 2.711 \\ &-2.110) \cdot 10^{-3} \end{aligned} \tag{11}$$

Fig. 5 contains the exact (Eq. (5)) and approximated equilibrium concentrations for $p = 3\,\text{bar}$ and $S/C = 3$. Deviations over the whole T_R and S/C-range are widely less than 1%, the maximal deviation is 2.2% for CH_4.

Fluid dynamics, i.e. transport delay and pressure drop are not included in the presented model, because these are small

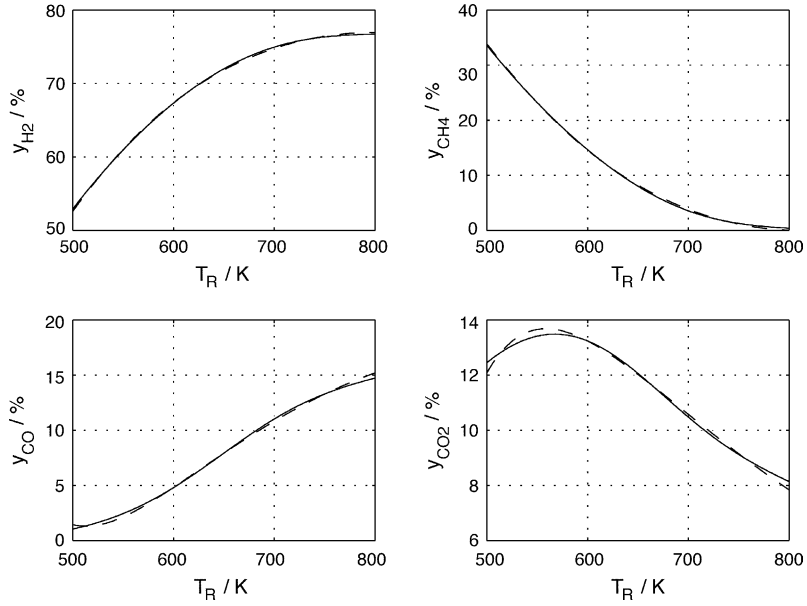

Fig. 5. Equilibrium concentrations for $p = 3$ bar and $S/C = 3$ (dry gas), the solid lines are calculated based on the minimum of the free enthalpy and the dashed lines are a polynomial approximation.

compared to the following plant components and therefore can be neglected.

The description above results in the following differential equations taking into account the heat capacities C, the heat exchange coefficients k, the burner gas flow rate $\dot{n}_B$, the flue gas flow rate $\dot{n}_F$ and the reformer gas flow rate $\dot{n}_R$:

wall:

$$C_W \frac{d}{dt} T_W = k_{GW}(T_G - T_W) - k_{WA}(T_W - T_A) - c_{p,B} \cdot \dot{n}_B (T_W - T_A) \quad (12)$$

ground plate:

$$C_G \frac{d}{dt} T_G = k_{BG}(T_B - T_G) - k_{GW}(T_G - T_W) + k_{FG} \cdot c_{p,F} \cdot \dot{n}_F (T_F - T_G) \quad (13)$$

burner:

$$C_B \frac{d}{dt} T_B = k_{FB}(T_F - T_B) - c_{p,B} \cdot \dot{n}_B (T_B - T_W) - k_{BR}(T_B^4 - T_R^4) - k_{BG}(T_B - T_G) \quad (14)$$

Table 2
Burner and flue gas flow rates depending on the burner state

Component	Burner off	Fan on	Burner on
$\dot{n}_{B,O_2}$	0	$2\lambda\dot{n}_V$	$2\lambda\dot{n}_V$
$\dot{n}_{B,N_2}$	0	$2\frac{79}{21}\lambda\dot{n}_V$	$2\frac{79}{21}\lambda\dot{n}_V$
$\dot{n}_{B,CH_4}$	0	0	$\dot{n}_V$
$\dot{n}_{F,O_2}$	0	$2\lambda\dot{n}_V$	$2(\lambda-1)\dot{n}_V$
$\dot{n}_{F,N_2}$	0	$2\frac{79}{21}\lambda\dot{n}_V$	$2\frac{79}{21}\lambda\dot{n}_V$
$\dot{n}_{F,CO_2}$	0	0	$\dot{n}_V$
$\dot{n}_{F,H_2O}$	0	0	$2\dot{n}_V$

evaporator:

$$C_E \frac{d}{dt} T_E = k_{RE}(T_R - T_E) + c_{p,F} \cdot \dot{n}_F (T_R - T_E) - r \cdot \dot{n}_{H_2O,i} - c_{p,H_2O} \cdot \dot{n}_{H_2O}(T_E - T_{H_2O}) - c_{p,CH_4} \cdot \dot{n}_{CH_4}(T_E - T_{CH_4}) - k_{EA}(T_E - T_A) \quad (15)$$

reactor:

$$C_R \frac{d}{dt} T_R = k_{BR}(T_B^4 - T_R^4) - k_{RE}(T_R - T_E) + c_{p,F} \cdot \dot{n}_F (T_{FG} - T_R) - \Delta h_0 \cdot \Delta\dot{n}_0 - \Delta h_1 \cdot \Delta\dot{n}_1 - c_{p,H_2O} \cdot \dot{n}_{H_2O}(T_R - T_E) - c_{p,CH_4} \cdot \dot{n}_{CH_4}(T_R - T_E) \quad (16)$$

Table 3
Model parameters

Parameter	Theoretical Value	Identified Value	Unit
C_W	9.2×10^3	7.27×10^3	J/K
C_B	0.56×10^3	0.22×10^3	J/K
C_E	9.35×10^3	5.42×10^3	J/K
C_G	3.5×10^3	2.44×10^3	J/K
C_R	4.65×10^3	3.61×10^3	J/K
v_0	–	-2.46×10^{-4}	mol/s
v_1	–	4.10×10^{-3}	mol V/s
λ	–	1.7	–
k_{BR}	$(0.78 \ldots 2.2) \times 10^{-9}$	1.32×10^{-9}	W/K^4
k_{BG}	0.83…2.8	4.50	W/K
k_{GW}	0.77…2.3	5.16	W/K
k_{EA}	0.11…2.7	0.439	W/K
k_{RE}	1.1…4.3	16.3	W/K
k_{WA}	0.32…6.4	1.16	W/K
k_{FB}	10	16.1	W/K
k_{FG}	0.5	0.30	–

with

$$T_F = T_B - \frac{\Delta h_C \cdot \dot{n}_{B,CH_4}}{c_{p,CH_4} \cdot \dot{n}_B + k_{FB}} \quad (17)$$

resulting from the energy balance of the combustion.

The burner gas flow rate $\dot{n}_B$ and the flue gas flow rate $\dot{n}_F$ depend on the burner valve position s_V and the burner state (fan and gas shut-off valve) and are listed in Table 2. Here v_0 and v_1 describe the linearized valve characteristics:

$$\dot{n}_V = v_0 + v_1 s_V \quad (18)$$

Obviously if the burner is off (left column) the flow rate is zero. If only the fan is on (this is the case at burner startup and shutdown) the air flow depends on the λ setting and the control valve position. If the burner is in operation, the right column is valid. The flue gas flow is calculated via the combustion reaction (3). Other than the above listed three operation modes do not occur.

The model is implemented in Matlab/Simulink.

4. Model parameters

Table 3 depicts all parameters with the theoretically calculated and identified (measured) values.

At first the parameters were theoretically determined. For some of them a minimal and a maximal value is given to account on uncertainty. For example consider the radiation from the burner to the reactor. The geometry of the burner

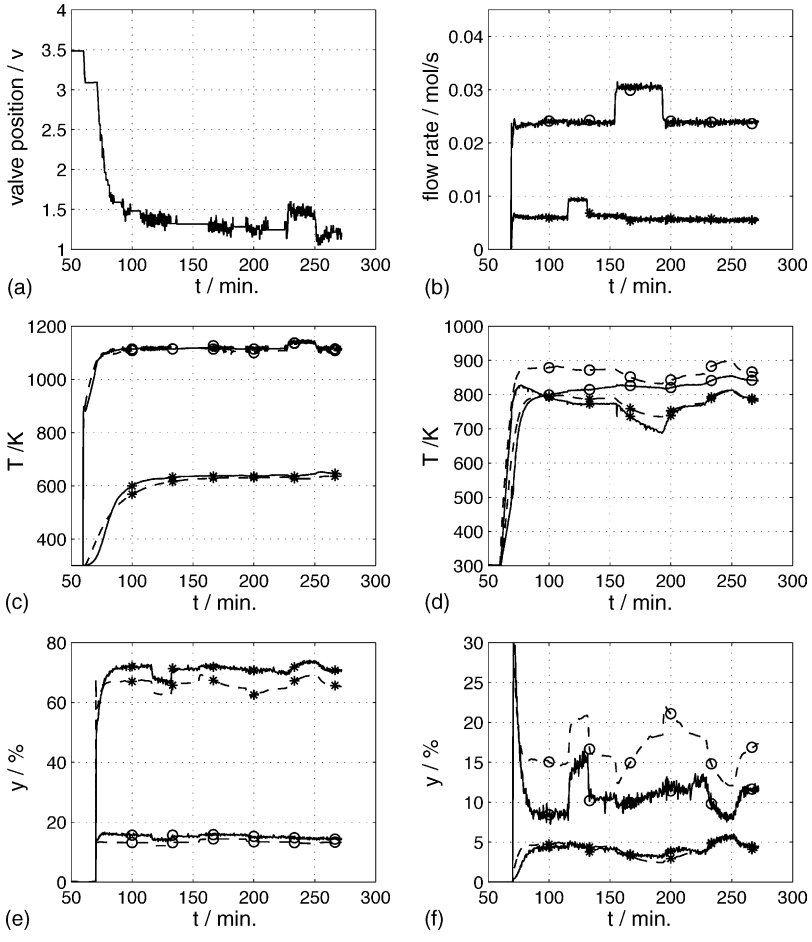

a)		valve position s_V		
b)	$*$	inlet gas flow rate $\dot{n}_{CH_4,i}$	$\circ$	inlet water flow rate $\dot{n}_{H_2O,i}$
c)	$*$	wall temperature T_W	$\circ$	burner temperature T_B
d)	$*$	evaporator temperature T_E	$\circ$	reactor temperature T_R
e)	$*$	H_2 concentration	$\circ$	CO_2 concentration
f)	$*$	CO concentration	$\circ$	CH_4 concentration

Fig. 6. Simulation with operating point at 40% of nominal power (solid lines are experimental data, dashed lines are simulated).

and the reactor are not as simple that a precise determination of k_{BR} is feasible. Moreover the effective emissivity could only be estimated within a certain range. The parameters of the burner valve, v_0 and v_1 are determined directly from measured burner gas flow rates at different valve positions. The λ value is calculated from the flue gas composition.

As simulations with these theoretical values did not show a perfect agreement with measured data, parameters were subsequently identified for the predefined model structure. The theoretical parameters were used as initial values for the identification algorithm `fmincon` [14]. The objective was to minimize the quadratic difference between simulation output and experimental data (consisting of T_B, T_E, T_W, y_{CH_4} and y_{CO} with appropriate scaling factors). We used an experimental data set comprising four sequences with different operating conditions.

5. Results

To demonstrate the model reliability, simulated and measured behaviour were compared. Figs. 6 and 7 show the simulation results of two different experiments. Both have a similar sequence: In diagrams (a) and (b) the model inputs are shown. These are the burner control valve position (a) and the water and natural gas flow rates (b). All further diagrams show the model outputs (dashed) in comparison to the respective measured values (solid). All relevant temperatures are in (c) and (d). The reactor temperature is not measured, but instead the reactor outlet temperature is shown. Note that the outlet temperature does only approximately and only during near steady-state operation match the actual reactor temperature. It is not meaningful during startup. The last two diagrams (e) and (f) contain the gas composition on a dry basis. As the concentrations depend on the reactor temperature they indirectly confirm the thermal model behaviour.

The first experiment (6) contains the reformer startup (at about 70 min) and operation at 40% of the nominal power. One after another the natural gas flow rate (at 120 min), the water flow rate (at 160 min) and the burner temperature were increased (at 230 min). The second experiment is similar, but at 70% of nominal power and with decreased flow rates.

The temperatures generally show a good agreement. Differences in the burner temperature (c) are hardly to notice.

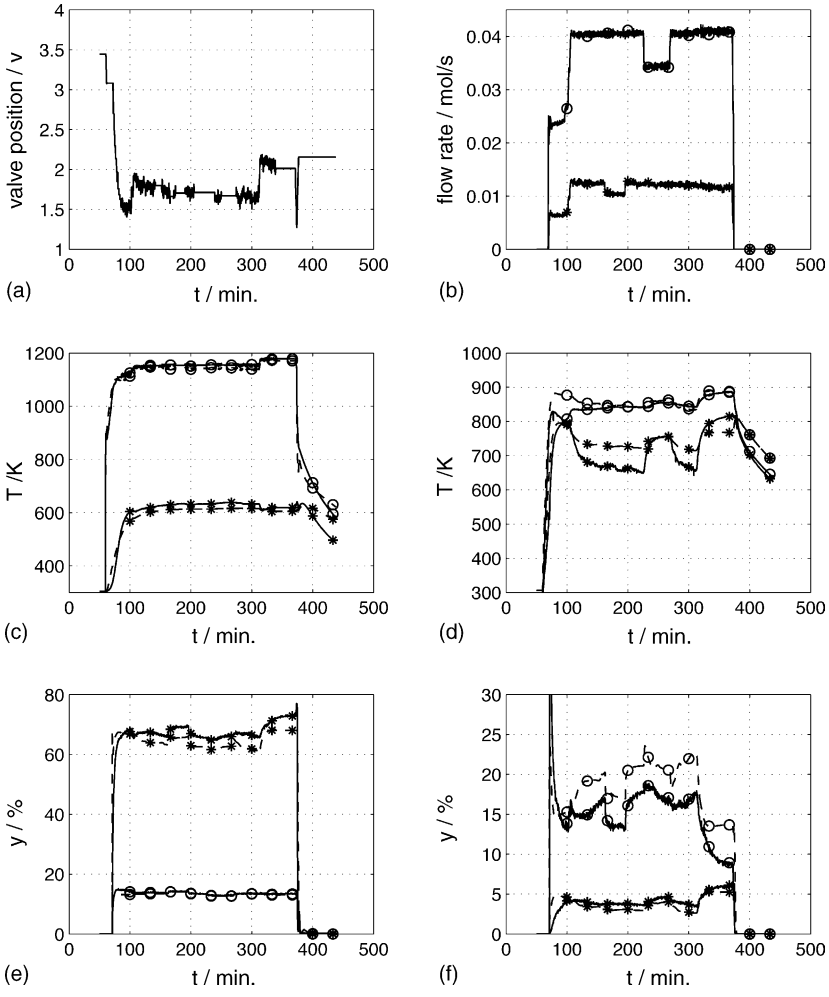

Fig. 7. Simulation with operating point at 70% of nominal power. See Fig. 6 for the legend.

Indeed during startup the simulated value is somewhat to high while for steady state conditions it is somewhat to low. At startup differences can be seen at the wall temperature (c): in reality this temperature rises with an obvious delay. The difference is caused by the lumped structure which cannot take into account temperature inhomogeneity during startup. As the wall temperature is not of major relevance for the system behaviour this deviation can be tolerated.

Diagram (d) depicts the evaporator temperature. The influence of changes of the water flow rate is smaller in the model than in reality. This can be explained by the reduction of the heat exchanger to one lumped element. But a more sophisticated model seems not necessary because this temperature is not an important value for the plant control.

The gas concentrations are also matched well (diagrams e and f), but obvious differences exist for methane.This is due to the high temperature sensitivity of the chemical equilibrium (see Fig. 5). Methane shows a strong temperature influence at normal operating conditions. The concentration doubles from 10 to 20% if the temperature decreases about 70 K, i.e. small deviations of the reactor temperature cause obvious changes in the methane concentration. Precise agreement of simulated and experimental CH_4-concentration therefore requires a precise temperature simulation. For online application this can be achieved by an observer, which combines the model with temperature sensor data.

The dynamic behaviour for both operating points is similar:

- Increasing the natural gas flow rate does hardly influence the thermal system but causes an increased outlet methane concentration.
- On the other hand increasing the water flow rate leads to lower evaporator and also reactor temperatures due to the higher evaporation heat. Initially the outlet hydrogen concentration is increased and the methane concentration decreased, but this is later on compensated by the lower temperature.
- Finally increasing the burner temperature results in a higher reactor temperature and therefore increased hydrogen and decreased methane concentration.

6. Conclusion

We described the derivation of a dynamic reformer model based on a theoretical, lumped element approach. The model structure and the parameter determination were explained. Experimental results of a demonstration plant were shown and compared with simulation results.

The presented data shows the good performance of our model despite its simple structure. Temperatures and gas compositions agree over a wide operation area including plant startup. It is also shown that for the outlet gas composition the assumption of chemical equilibrium holds.

References

[1] A. Heinzel, et al., Hydrogen generation by small scale reformers – the activities of Fraunhofer ISE, HYFORUM 2000. EFO Energy Forum, Bonn, 2000.
[2] J. Larminie, A. Dicks, Fuel Cell Systems Explained, Wiley, Chichester, 2000.
[3] L. Ljung, T. Glad, Modeling of Dynamic Systems, Prentice Hall, Englewood Cliffs, N.J London, 1994.
[4] System Identification Toolbox User's Guide, Version 5, The MathWorks Inc., 2000.
[5] A.M. Meziou, I.M. Alatiqi, Identification and control of an industrial steam reforming plant, Can. J. Chem. Eng. 72 (April 1994).
[6] M.P. Nielsen, S.K. Kær, Modeling a PEM Fuel Cell Gas Reformer, ECOS 2003 Copenhagen, Denmark, June 2003.
[7] C. Maume, Systemanalyse und Simulation eines Brennstoffzellen-Hybrid-Fahrzeugs mit autothermer Methanolreformierung, PhD Thesis, TU München, 2002.
[8] M.V. Twigg (Ed.), Catalyst Handbook, 2 ed., Manson Publ., London, 1996.
[9] A. Lamm, Modellmäßige Beschreibung und Simulation eines Heizsystems mit keramischem Strahlungsbrenner, PhD Thesis, Forschungszentrum Jülich, 1995.
[10] Verein Deutscher Ingenieure (Ed.), VDI-Wärmeatlas, Springer, 2002.
[11] J. Mathiak, Verfahrensanalyse zur dezentralen Hausenergieversorgung auf Basis von PEM-Brennstoffzellen, PhD Thesis, Universität Duisburg-Essen, 2002.
[12] Z.-W. Liu, K.-W. Jun, H.-S. Roh, S.-E. Park, J. Power Sources 111 (2002) 283.
[13] W.J. Moore, Physikalische Chemie, 4. ed., de Gruyter, Berlin, New York, 1986, p. 328.
[14] The Optimization Toolbox User's Guide, Version 2.1, The MathWorks Inc., 2001.